Different Ways of Framing Event Attribution Questions: The Example of Warm and Wet Winters in the United Kingdom Similar to 2015/16

NIKOLAOS CHRISTIDIS, ANDREW CIAVARELLA, AND PETER A. STOTT

Met Office Hadley Centre, Exeter, United Kingdom

(Manuscript received 13 July 2017, in final form 28 November 2017)

ABSTRACT

Attribution analyses of extreme events estimate changes in the likelihood of their occurrence due to human climatic influences by comparing simulations with and without anthropogenic forcings. Classes of events are commonly considered that only share one or more key characteristics with the observed event. Here we test the sensitivity of attribution assessments to such event definition differences, using the warm and wet winter of 2015/16 in the United Kingdom as a case study. A large number of simulations from coupled models and an atmospheric model are employed. In the most basic case, warm and wet events are defined relative to climatological temperature and rainfall thresholds. Several other classes of events are investigated that, in addition to threshold exceedance, also account for the effect of observed sea surface temperature (SST) anomalies, the circulation flow, or modes of variability present during the reference event. Human influence is estimated to increase the likelihood of warm winters in the United Kingdom by a factor of 3 or more for events occurring under any atmospheric and oceanic conditions, but also for events with a similar circulation or oceanic state to 2015/16. The likelihood of wet winters is found to increase by at least a factor of 1.5 in the general case, but results from the atmospheric model, conditioned on observed SST anomalies, are more uncertain, indicating that decreases in the likelihood are also possible. The robustness of attribution assessments based on atmospheric models is highly dependent on the representation of SSTs without the effect of human influence.

1. Introduction

Attribution of weather and climate extremes assesses in a quantitative manner the extent to which causal factors (most commonly anthropogenic climate change) may have altered certain characteristics such as their likelihood or magnitude (Stott et al. 2016). Rapid scientific advances in this area helped dispel initial skepticism over the feasibility of such an undertaking and the potential of event attribution was recently acknowledged by the United States (National Academies of Sciences, Engineering, and Medicine 2016). Driven by a high demand for attribution information from scientists, decision makers and the public, the *Bulletin of the American Meteorological Society* (*BAMS*) has been publishing an annual special report on the State of the Climate that reviews extreme events of the previous year in the context of climate variability and change (Peterson et al. 2012, 2013; Herring et al. 2014, 2015, 2016a). Having reached its sixth issue, the report has demonstrated the proliferation of attribution methods and illustrated their application to over 100 events. Besides the relatively easier cases of temperature extremes for which the effect of human influence is most likely to be detected, the anthropogenic signal has also been shown to alter the characteristics of rainfall extremes and storms (e.g., Schaller et al. 2016), droughts (Lott et al. 2013), tropical cyclones (Zhang et al. 2016), hurricane-related inundations (Sweet et al. 2013), and so on. Of course unforced climatic variability is still a crucial factor that may dominate over any anthropogenic effect and hinder its detection, as was the case in about 35% of the studies published in the *BAMS* reports. International research initiatives like the Climate of the 20th Century Plus attribution project (C20C+; http://portal.nersc.gov/c20c/) have promoted research via collaborative work, while the recent European project European Climate and Weather Events: Interpretation and Attribution (EUCLEIA) took a step further, integrating event attribution into a quasi-operational framework. Fully operational systems issuing attribution assessments on a regular basis have the

Corresponding author: Nikolaos Christidis, nikos.christidis@metoffice.gov.uk

DOI: 10.1175/JCLI-D-17-0464.1

potential to become the go-to place for robust scientific information in the aftermath of high-impact events and to play a key role in developing climate services.

Risk-based attribution analyses derive changes in characteristics (e.g., likelihood) of extreme events by comparing their distribution in the real world against their distribution in a hypothetical natural world without human influence on the climate. This simple concept was introduced by Stott et al. (2004) in his study of the 2003 summer heatwave in Europe. Different methodologies employ essentially the same concept, but use different tools to construct the aforementioned distributions. For example, numerous studies employ large ensembles of simulations generated with atmospheric models (Pall et al. 2011; Christidis et al. 2013; Black et al. 2016), while others employ coupled model simulations (Christidis and Stott 2016; Lewis and Karoly 2015) or long observational records (Vautard et al. 2015; van Oldenborgh et al. 2015). Multimethod analyses have also been undertaken (King et al. 2015; Otto et al. 2015a; van der Wiel et al. 2017). Methodological variants introduce subtle differences in the framing of the attribution question. For example, analyses with atmospheric models may estimate the changing likelihood of an event given the observed state of the ocean at the time it occurred (prescribed through the boundary conditions), while studies with coupled models sample the entire range of oceanic variability. It becomes evident from this example that despite the widespread use of the term ''event attribution,'' attribution studies do not represent an actual event with all the unique conditions in which it occurred. Instead, ''classes of events'' are employed that only share some characteristics with the event under consideration.

The simplest class of events in attribution studies defines extremes in relation to a pre-specified threshold of the relevant climatic variable. This was the case in Stott et al. (2004), where severe summer heatwaves in Europe were defined as exceedances of the second highest summer temperature in the instrumental record. While thresholds are invariably employed in risk-based analyses, additional constraints may be introduced to create classes of events that share more characteristics with the event under consideration. As already mentioned, studies with atmospheric models can condition the estimated change in the risk of extremes to the observed SSTs and so alter the event's definition from simply crossing a threshold to crossing a threshold under the observed state of the ocean. This conditioning may be critical in regions where the occurrence of extremes is strongly influenced by the SSTs (Seager and Hoerling 2014; Christidis and Stott 2014). When other known drivers of extremes come into play, a similar conditioning may be introduced. Examples include attribution studies that account for the phase of El Niño–Southern Oscillation (ENSO; King et al. 2016; Karoly et al. 2016), the dominant atmospheric circulation pattern (Christidis and Stott 2015; Yiou and Cattiaux 2014), etc. Such studies often investigate not only the anthropogenic influence on extremes, but also the contribution from the additional driving factor. It is then possible that analyses of the same event may yield different results, only because the attribution is conditioned on different factors. In this paper we start from a basic class of events, namely warm and wet U.K. winters with the temperature and rainfall exceeding pre-specified values that describe climatological extremes, as was the case in December 2015–February 2016 (DJF 2015/16), and then alter the attribution question by conditioning our assessment on a host of possible driving factors.

It should be noted that the framing of the attribution question may also differ in other ways not considered here. The likelihood of extremes may for instance be sensitive to the specification of the threshold used to define extreme events or the region considered in the analysis, as discussed in Otto et al. (2015b) and Angélil et al. (2018). Analyses of the same event may also employ different variables to describe it. In a later commentary Otto (2016) also pointed out that the overall change in the risk of extremes begs consideration of both thermodynamic and dynamic changes. The latter arise from anthropogenic influence on the atmospheric circulation and, although they are generally less easily detected, their contribution has been considered in the literature (e.g., Schaller et al. 2016; Vautard et al. 2016). Here we only employ a single threshold to define extreme events and do not attempt a separation of the thermodynamic and dynamic effects, but focus on the overall change in the likelihood of warm and wet winters in the United Kingdom conditioned on different factors. More specifically, we set out to estimate the likelihood of extreme events in the general case (i.e., due to anthropogenic forcings only), as well as the effect that the following additional factors have on the likelihood (all these factors describe different characteristics of winter of 2015/16):

- SST anomaly patterns observed in DJF 2015/16,
- strong El Niño conditions,
- southwesterly atmospheric flow, and
- strong westerly phase of the quasi-biennial oscillation (QBO).

Some of these factors were also examined in the study of the 2015/16 event by Scaife et al. (2017) and were found to increase predictability, at least when acting in synergy as part of wider teleconnections. Considering the same

event in this paper offers a complementary attribution perspective to the seasonal forecasting's frame of reference. Although we do not expect all factors examined here to have equally contributed to the event, considering a range of possible drivers, from primary to secondary, helps to investigate better the sensitivity to framing. Finally, unlike forecast simulations, the model simulations in attribution studies are generally not initialized. The effect of using uninitialized model runs will also be examined.

The remainder of the paper is structured as follows: Section 2 briefly describes the event under consideration and presents the data and the different methodological approaches used in this study. Section 3 lists various evaluation tests applied to the models to assess their suitability for event attribution. Results are presented in section 4. Some discussion on the main findings and concluding remarks are given in section 5.

2. Attribution of the U.K. winter of 2015/16: Methods and data

a. The event

Time series of the winter mean temperature and rainfall averaged over the United Kingdom (48°–60°N, 10°E–3°W) are constructed using the HadCRUT4 (Morice et al. 2012) and GPCC (Schneider et al. 2014) datasets (Fig. 1) and show that DJF 2015/16 was the fourth warmest and third wettest winter since 1900. The event developed under the synergy of known predictive factors (Scaife et al. 2017), namely the presence of a very strong El Niño, a strong westerly phase of the QBO (Baldwin et al. 2001), and a vigorous stratospheric polar night jet early in the season. The interplay between these factors favors extratropical cyclogenesis, which led to the 2015/16 warm and wet conditions in the United Kingdom, skillfully predicted (Scaife et al. 2017) by the Met Office's Global Seasonal Forecast System version 5 (GloSea5; MacLachlan et al. 2015). Figure 2a shows the evolution of the QBO index in recent decades using zonal wind data at 30 hPa over the equator from NOAA/CPC (http://www.cpc.ncep.noaa.gov/data/indices/). The index was near its positive peak during the winter of 2015/16 (highlighted in red on the time series), indicating strong westerly winds, but, interestingly, the QBO failed to swing into its easterly phase later in the year (Newman et al. 2016). Strong El Niño conditions during the winter season are evident in the time series of the oceanic Niño index (ONI) for DJF (Fig. 2c), also constructed with NOAA/CPC data. ONI is computed as 3-month SST anomalies in the Niño-3.4 region relative to 30-yr base periods updated regularly to minimize the effect of long-term warming. In this study we use an SST-based index for ENSO, rather than a pressure-based one, as the latter would involve a retrieval of a large amount of pressure data from a large number of models. Instead, we construct modeled ONI data from near-surface air temperatures (also used in the attribution analysis) rather than SSTs. Using simulations from a single model (HadGEM2-ES) we confirmed that ONI values retrieved with near-surface air temperatures and oceanic temperatures are almost identical (correlation coefficient greater than 0.99). While the unique characteristics of the event, given the state of the atmosphere and the ocean at the time it occurred, are crucial in seasonal forecasting, event attribution, as already mentioned, is concerned with broader classes of events. The likelihood of such events is derived from distributions constructed with model simulations. In this study we use experiments with different external forcings carried out with both atmospheric and atmosphere–ocean coupled models.

b. Coupled models

Coupled models sample in principle the entire range of internal variability and therefore yield broad distributions of climatic variables (e.g., temperature for the study of heatwaves), which in turn provide estimates of the likelihood of extremes in the "general case" (i.e., under any possible conditions). This approach has been employed in event attribution to estimate the change in the risk of extremes due to human influence, using either the raw modeled response to climatic forcings (Lewis et al. 2014) or a refined scaled response that matches better the observations (Christidis et al. 2015). Here we use multimodel ensembles from 38 models that contributed data to phase 5 of the Coupled Model Intercomparison Project (CMIP5; Taylor et al. 2012).

Simulations with all historical forcings are used to represent the actual climate (ALL). These include both anthropogenic influences (emissions of well-mixed greenhouse gases, aerosols, and ozone, as well as land-use changes) and natural forcings (changes in volcanic aerosols and the solar irradiance). Temperature and rainfall distributions representative of the U.K. climate in winter 2015/16 are constructed by extracting model data over a 10-yr period (2010/11–2019/20) centered on the reference year. As we have 86 ALL simulations in total (Table 1), we get samples of 860 winters with which we make probability density functions (PDFs) for 2015/16. These provide estimates of the likelihood of extremes in the actual world in the general case. Similarly, distributions for the natural climate (NAT) are made using model experiments without the effect of anthropogenic forcings. Here, we use 35 "control" simulations

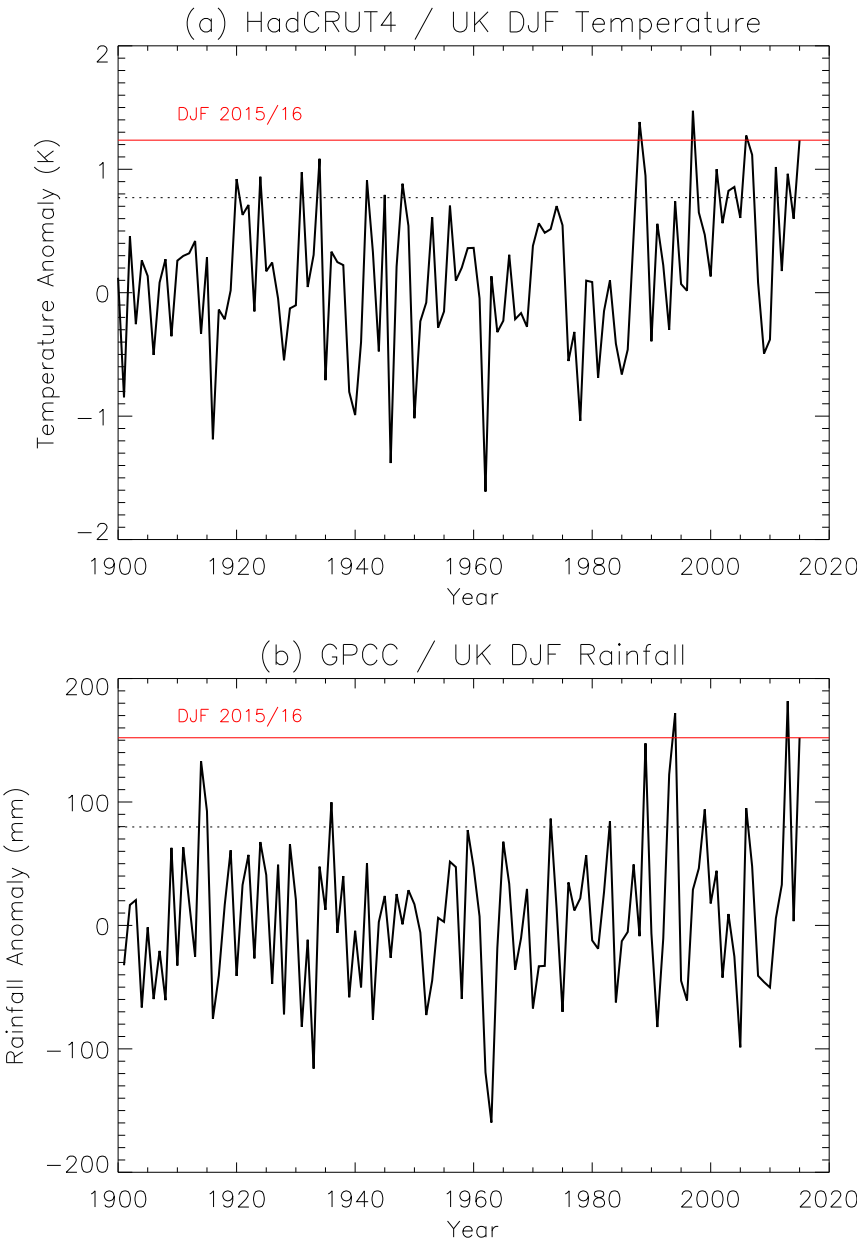

FIG. 1. Time series of winter mean (a) temperature and (b) rainfall anomalies relative to 1961–90 averaged over the U.K. region (48°–60°N, 10°E–3°W). The time series were constructed with the HadCRUT4 and GPCC datasets. The red lines mark the observed values in winter 2015/16 and the dotted lines the 1-in-10-year events during 1961–90. A weak positive correlation between winter temperature and rainfall is found (correlation coefficient 0.12).

representing the preindustrial climate (Table 1). The disadvantage of using control simulations is that they do not include the effect of natural forcings, which, however, is generally weaker and short-lived and is not expected to have strong influence on the distributions. Although CMIP5 simulations with natural forcings are available, the majority of them end in year 2012 and are therefore not useful for this work. The advantage of the control experiment is that its simulations are long (typically multicentennial) and can thus provide large samples of data. Sixty-year-long segments are extracted from the simulations, representative of the NAT climate in 1961–2020, from which we again use the last 10 years to represent the climate in winter 2015/16. The reason we extract long segments is that we use the first 30 years (representing the period 1961–90 in the preindustrial

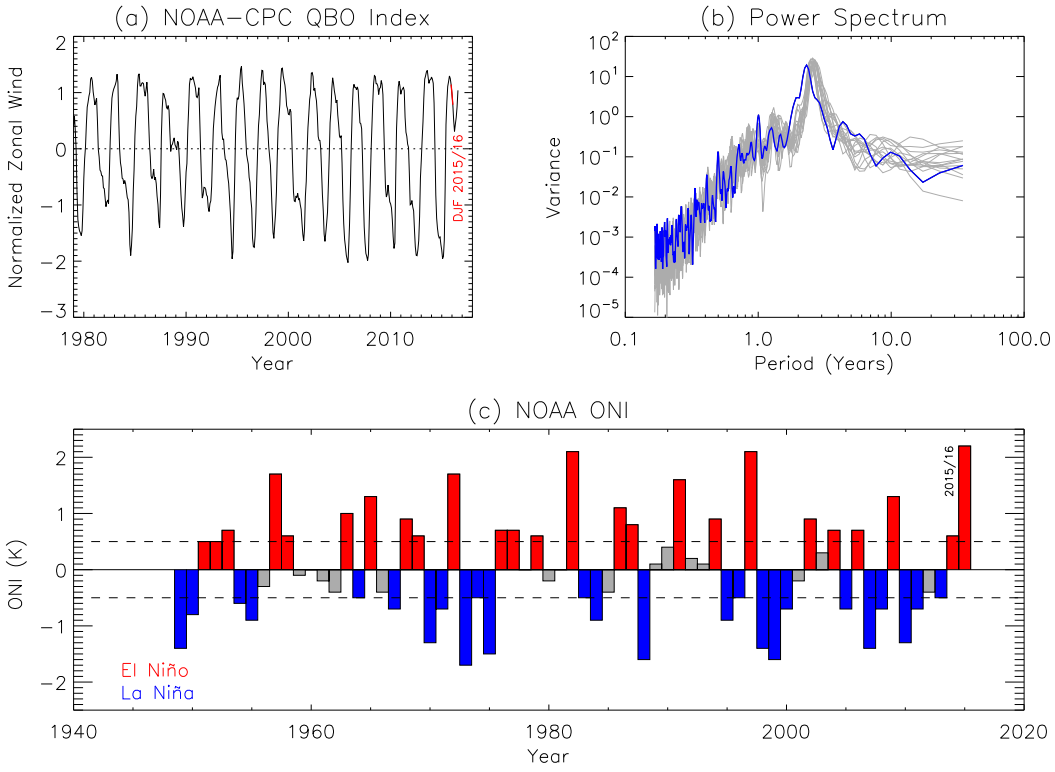

FIG. 2. (a) Time series of the monthly QBO index produced with NOAA/CPC data. The winter of 2015/16 is marked in red. (b) Power spectra for the QBO index during 1960–2013 based on NOAA/CPC data (blue line) and the 15 HadGEM3-A simulations with ALL forcings (gray lines). (c) Time series of the DJF mean ONI from NOAA/CPC data. Red, blue, and gray bars indicate El Niño, La Niña, and neutral ENSO conditions. Horizontal dashed lines mark the ±0.5-K ONI values, commonly used to differentiate between different ENSO phases. Testing whether the slope of least squares fits is significantly different than zero indicates no significant trends in the observed QBO and ONI time series (p values greater than 0.1).

climate) as a base period to express temperature and rainfall as anomalies. The use of anomalies enables comparison with observational data and helps remove model biases, which is important when creating a multimodel ensemble. The control simulations provide large samples of 3060 winters in total representative of DJF 2015/16 (Table 1) in the NAT world. It should be noted that all simulations in this study are given an equal weight despite the fact that the selected models provide different number of simulations for each experiment. Rather than investigating the role of model dependence (Hauser et al. 2017), here we solely focus on the framing effect. The combined data we use are evaluated in section 3 and found to be suitable for our attribution analysis.

c. *Atmospheric model*

We use simulations from the Hadley Centre's event attribution system (Christidis et al. 2013) built on the atmospheric model HadGEM3-A (Hewitt et al. 2011). The model was upgraded during the EUCLEIA project and now features a high horizontal resolution of about 60 km and 85 vertical levels (Ciavarella et al. 2018). The attribution system currently runs on a seasonal cycle and every quarter produces large ALL and NAT ensembles for the study of events in the preceding season. Unlike the CMIP5 models used in this paper, the NAT simulations with the atmospheric model include the effect of natural forcings. The Hadley system provided simulations for numerous studies of different types of extremes, several of which published in the annual special reports of *BAMS*. In this study we use the ALL and NAT ensembles for winter 2015/16, each comprising 105 simulations. In addition, we also employ, as explained later, smaller 15-member ALL and NAT ensembles of multidecadal simulations that cover the period 1960–2013. The longer runs for the actual climate are also used for model evaluation.

Atmospheric simulations require boundary conditions of prescribed SSTs and sea ice cover. The ALL experiment employs observations from the HadISST dataset (Rayner et al. 2003). The representation of

TABLE 1. CMIP5 models used in the analysis. The number of ALL simulations provided by each model is shown together with the number of 60-yr-long segments extracted from the CONTROL experiment. The total number of winters extracted from the simulations and used to construct distributions for winter 2015/16 with and without human influence is reported on the last row. The ALL simulations were extended following the representative concentration pathway 4.5 (RCP4.5). As differences in climate trends between RCPs become evident later in the century, results presented here are not sensitive to the RCP choice. (Expansions of acronyms are available online at http://www.ametsoc.org/PubsAcronymList.)

	ALL	CONTROL
Model	Ensemble size	No. of segments extracted
ACCESS1.0	1	8
ACCESS1.3	1	8
BNU-ESM	1	9
CCSM4	6	17
CESM1-BGC	1	8
CESM1-CAM5	3	5
CESM1-WACCM	1	3
CMCC-CM	1	5
CMCC-CMS	1	8
CNRM-CM5	1	14
CSIRO-Mk3.6.0	10	8
CanESM2	5	16
EC-EARTH	6	7
FIO-ESM	3	13
GFDL-CM3	1	—
GFDL-ESM2G	1	—
GFDL-ESM2M	1	—
GISS-E2-H	5	8
GISS-E2-H-CC	1	4
GISS-E2-R	6	14
GISS-E2-R-CC	1	4
HadGEM2-AO	1	11
HadGEM2-CC	1	4
HadGEM2-ES	4	9
IPSL-CM5A-LR	4	16
IPSL-CM5A-MR	1	4
IPSL-CM5B-LR	1	4
MIROC-ESM	1	10
MIROC-ESM-CHEM	1	4
MIROC5	3	11
MPI-ESM-LR	3	16
MPI-ESM-MR	3	16
MRI-CGCM3	1	8
NorESM1-M	1	8
NorESM1-ME	1	4
BCC-CSM1.1	1	8
BCC-CSM1.1-M	1	6
INM-CM4.0	1	8
Total number of years	860	3060

cooler oceans in the NAT climate requires an estimate of the anthropogenic change in the SSTs (delta SST) to be subtracted from the observations. Deriving this estimate constitutes the largest uncertainty in studies with atmospheric models. Typically, delta SST estimates have been obtained from experiments with coupled models (Pall et al. 2011; Christidis et al. 2013), as was also done in this study. More specifically, we use the average modeled anthropogenic change in SST across 51 simulations with 19 CMIP5 models, a common benchmark for several attribution systems participating in the C20C+ project (http://portal.nersc.gov/c20c/experiment.html). Simple empirical relationships are also used to adjust the sea ice in the NAT simulations accordingly as in previous work (Christidis et al. 2013). The DJF mean SSTs in the model runs for winter 2015/16 are shown in Figs. 3a and 3b for the ALL and NAT experiment respectively. The delta SST pattern is illustrated in Fig. 3c. Pattern uncertainty is sometimes represented by producing several versions of the NAT experiment, with delta SST patterns from different individual models (e.g., Pall et al. 2011; Schaller et al. 2014). This, however, is a computationally expensive approach. The use of a single pattern from a multimodel ensemble, as in this study, is deemed a good compromise, as it could minimize individual model errors. Alternatively, observationally derived delta SST patterns have also been proposed (Christidis and Stott 2014; Takayabu et al. 2015; Shiogama et al. 2014), whereby linear trends in SST are removed at each grid point of HadISST. A possible caveat in the latter approach is that the trends may to some extent be influenced by long-term variability. Nevertheless, the HadISST record may be considered sufficiently long (over 140 years) to minimize the impact of variability on the delta SST pattern. The observationally derived pattern for DJF 2015/16 (not used in this analysis) is shown in Fig. 3d. The modeled and observational patterns both show an overall warming, which however is much stronger according to the models (global mean warming of 0.87 K estimated with CMIP5 models and 0.57 K estimated with HadISST). The patterns also display different characteristics that may be important in regions strongly influenced by the ocean (Christidis and Stott 2014), as will also be discussed later. The SSTs prescribed in the NAT simulations retain the El Niño signal (Fig. 2b) as well as the broad general characteristics of the observed patterns (e.g., the cooling region south of Greenland). The northernmost parts of the Atlantic, however, display a warming in the ALL experiment, but a strong cooling in the NAT experiment, possibly linked to the Arctic amplification effect (Pithan and Mauritsen 2014; Serreze and Barry 2011). Unlike the ENSO phase that is prescribed through the boundary conditions, the NAT simulations do not retain the observed phase of the QBO, as they grow out of phase with the observations a few years after their

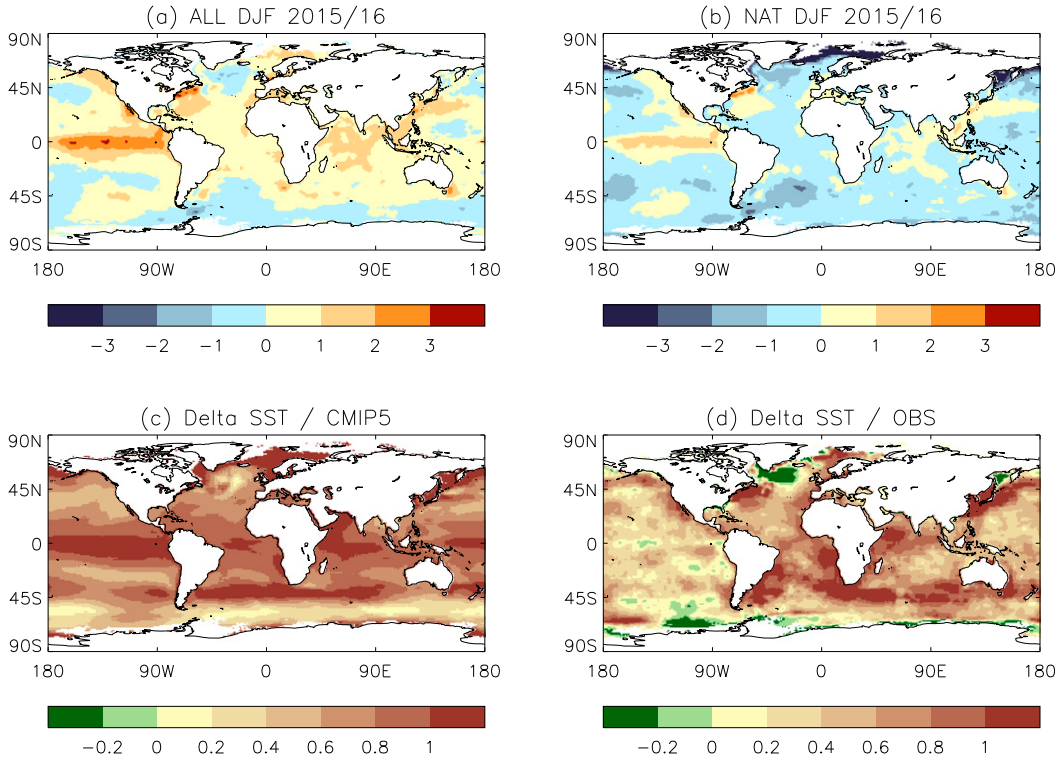

FIG. 3. (a) DJF mean SSTs from monthly HadISST values used as boundary conditions in the ALL experiment. (b) As in (a), but for the NAT experiment. In this case, modeled monthly delta SST estimates were subtracted from the HadISST data. All SSTs are anomalies relative to 1961–90. (c) The DJF mean delta SST pattern from monthly model-based estimates of the SST change due to human influence used in this study. (d) The DJF mean delta SST pattern estimated from HadISST observations after removing the trend.

start. However, power spectra of the QBO index produced with the 15 multidecadal simulations of the ALL experiment (Fig. 2b) show that the model captures well the periodicity of the QBO.

d. Framing

Samples of simulated data from the ALL and NAT experiments render distributions of winter temperature and precipitation over the United Kingdom with and without the anthropogenic effect. Warm and wet events are defined relative to a temperature anomaly of 0.77 K and a total winter precipitation anomaly of 79.75 mm, corresponding to 1-in-10-year events during the 1961–90 climatological period. Using such moderate thresholds instead of the actual 2015/16 observations (red lines in Fig. 1) to define extremes provides a more general event description and avoids the difficulty of calculating very small probabilities associated with very large uncertainties. The selected thresholds define broad classes of events that only share one basic characteristic with the winter 2015/16 (i.e., the exceedance of the specified threshold anomalies). The choice of the 1961–90 baseline is common in attribution studies, as observational datasets like HadCRUT4 provide anomalies relative to this period. As in previous work, we employ the generalized Pareto distribution (GPD) to estimate probabilities of extremes when the threshold lies in the tail of the distribution and a Monte Carlo bootstrap procedure to compute uncertainties (Christidis et al. 2013). Taking a step further, we subsequently define other classes of events that share some more characteristics with the reference event. This is done by subsampling the modeled data (i.e., extracting only winters that feature the characteristic under consideration). As an example, Fig. 4 illustrates how the effect of the characteristic winter circulation in DJF 2015/16 can be investigated. The 500-hPa geopotential height map from the NCEP–NCAR reanalysis (Kalnay et al. 1996) displays a large-scale cyclonic circulation northwest of the United Kingdom (Fig. 4a) and an associated westerly/southwesterly flow over the country, which transports warm and humid air from warmer parts of the Atlantic. As in Christidis et al. (2013, 2015), we use flow pattern correlations greater than 0.6 over the wider U.K. area (black box in Fig. 4) to select modeled winters with circulation similar to 2015/16. The 105 winters from the

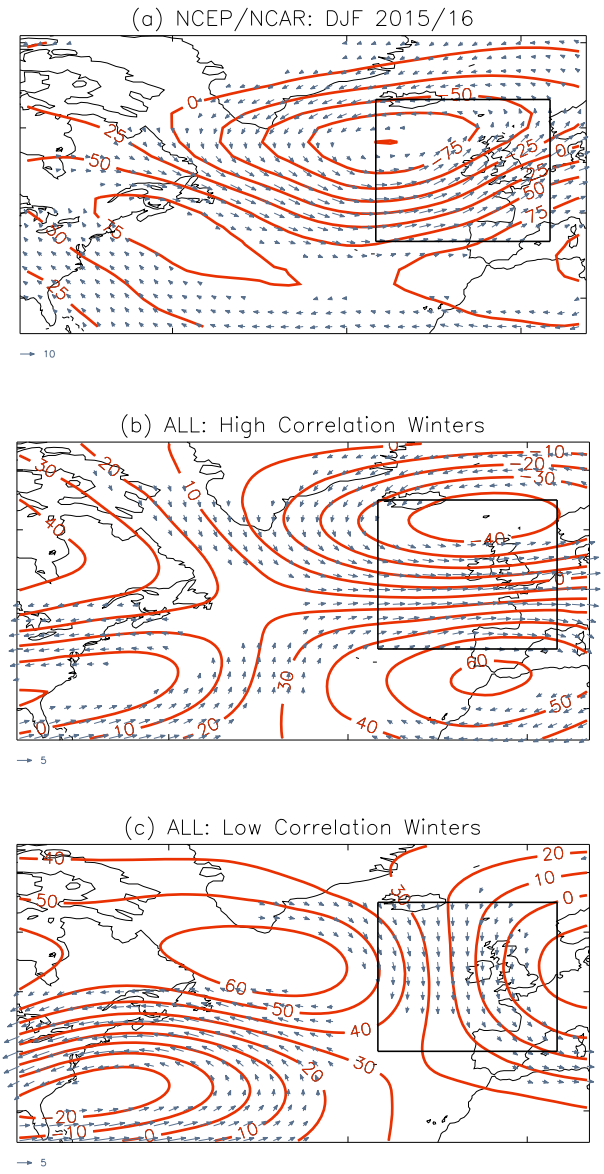

FIG. 4. Maps of the 500-hPa geopotential height (red contours) and wind (blue vectors) in a wide North Atlantic region for winter 2015/16 from (a) the NCEP–NCAR reanalysis and the mean of HadGEM3-A simulated winters with correlations (b) greater than 0.6 and (c) less than 0.6 with the reanalysis pattern over the region marked by the black box.

ALL simulations with HadGEM3-A are so partitioned between 29 high-correlation and 76 low-correlation events (Figs. 4b,c). The NAT simulations can be partitioned in a similar way. Subsampling allows us to examine 1) how the circulation affects the likelihood of extremes (by comparing high- and low-correlation events in the actual climate) and 2) how anthropogenic forcings affect the likelihood of extremes developing under specific synoptic conditions (e.g., by comparing only high-correlation events in the ALL and NAT experiments). One disadvantage of subsampling is that the uncertainty in probability estimates derived from smaller samples tends to increase.

In this study we compute the probability, or return time (inverse probability), of warm and wet U.K. winters with and without human climatic influence, using whole samples of simulated winters, or subsamples, in order to create certain classes of events as explained above. The classes of events we consider are listed below:

- The general case. All simulated winters from the coupled model experiments are used to construct temperature and rainfall distributions that span the entire variability range and yield the likelihood of extremes under any possible conditions. Years 2010/11–2019/20 are extracted from the ALL simulations to represent the 2015/16 climate and a number of winters are also extracted from control simulations, as explained earlier, without human climatic influence. In total, we obtain samples of 860 and 3060 winters from experiments with and without the anthropogenic effect.
- Events conditioned on the phase of ENSO. The samples of DJF temperature and rainfall used in the general case are grouped according to the phase of ENSO in model simulations. ONI values greater than 0.5 correspond to El Niño conditions and less than −0.5 to La Niña conditions. We end up with 353 El Niño and 166 La Niña winters for the actual climate and 832 El Niño and 845 La Niña winters for the natural climate.
- Events conditioned on the state of the ocean. Atmospheric model simulations of winter 2015/16 provide the likelihood of extreme events developing under the characteristic SST patterns observed that year. There are 105 simulations for each of the ALL and NAT experiment.
- Events conditioned on the state of the ocean and the phase of the QBO. The 105 winters from each HadGEM3-A experiment are partitioned between those that have a strong positive QBO phase as in 2015/16 (index values greater than 0.7) and those that do not. There are 29 winters with strongly positive QBO in the ALL climate and 17 in the NAT climate.
- Events conditioned on the state of the ocean and the atmospheric circulation. The 105 winters from each HadGEM3-A experiment are partitioned between those that have high correlations with the circulation pattern over the United Kingdom in winter 2015/16 (correlation coefficient greater than 0.6) and those that do not. There are 29 winters with high correlations in the ALL climate and 43 in the NAT climate.

All approaches listed above provide valid ways of looking at the same event, but frame the attribution question slightly differently. While focusing on the

precise event with all its unique characteristics is imperative in forecasting, events are more loosely defined in attribution research using classes, which marks a crucial and sometimes confusing difference in terminology. Although one could criticize attribution studies for not describing the event in all its details, it could also be argued that considering classes of events may provide more useful information to decision makers. For example, if exceeding a critical temperature threshold triggers catastrophic heatwaves in a region, then changes in the frequency of such threshold exceedances would be of greater interest to adaptation planers than changes in the likelihood of a single heatwave event that developed under a very specific set of conditions. Another important difference between attribution and forecasting is the effect of initialization. While retaining memory of the initial conditions in model simulations could strongly affect forecasting skill, attribution simulations produced with the Hadley system are uninitialized and simply extended from the previous set of runs as new ensembles are generated every quarter. We test the effect of initialization by comparing temperature and rainfall distributions constructed with the 105 ALL HadGEM3-A simulations for winter 2015/16 with distributions from 72 initialized runs produced by the GloSea5 system for the same season. The GloSea5 simulations include two runs per day for all days in November 2015, as well as three hindcast runs produced four times in the same month. Before proceeding with the results of our analyses, we first consider the suitability of the models used in this work for event attribution and present a number of simple evaluation assessments in the next section.

3. Model evaluation

Event attribution relies largely on climate models, which need to be carefully evaluated to ensure they are fit for the purpose. Evaluation may encompass a range of tests against independent observational (or in some cases reanalysis) data that indicate whether models reproduce well the statistics and climatology of the relevant climatic variables and their extremes, as well as other processes or drivers of extremes pertinent to the case under investigation. The Hadley attribution system was rigorously evaluated during the course of the EUCLEIA project and found to be an excellent tool for the attribution of several types of European extremes (Vautard et al. 2018). Studies of individual events, however, require tailored assessments of the models used, as model performance may vary between different regions and extreme types (Christidis et al. 2013). When the ability of the model to capture predictable features of events is important, then reliability diagrams, popular in seasonal forecasting, may also be employed (Lott et al. 2014). Here, however, we are more concerned about classes of events than the models' forecasting skill. We apply a number of well-established tests (examples found in studies with the Hadley system in the special reports of *BAMS*) to assess whether HadGEM3-A and the CMIP5 models reproduce well the winter temperature and rainfall climatological distributions in the United Kingdom and their variability and extremes, as well as the influence of ENSO, the QBO, and the 2015/16 circulation pattern. Here we evaluate the CMIP5 multimodel ensemble as a whole, instead of looking at individual models. Alternatively, only the best models could have been utilized in the analysis, but since the performance of the overall ensemble is found to be good, we decided to proceed with all models and so take advantage of larger sample sizes, which help estimate probabilities with greater confidence.

The climatological distributions of winter temperature and precipitation in the United Kingdom during the period 1960–2013, which is common to all datasets, are illustrated in Fig. 5. The similarity between the observed and modeled PDFs is tested with a two-sided Kolmogorov–Smirnov (KS) test. The null hypothesis stating that the distributions are not significantly different can be rejected at the 10% level (p values greater than 0.1). The models also yield a realistic representation of the observed variability across different time scales, as suggested by power spectra analyses (Figs. 6a,b), a common tool in model evaluation (Gillett et al. 2000). The observed spectra lie within the range of spectra produced with individual HadGEM3-A and CMIP5 simulations. As expected, the range of the CMIP5 models is wider because of the much larger number of simulations that are able to capture more extreme values. We next use the GPD distribution to zoom in on the warm and wet tails of the climatological PDFs shown in Fig. 5. The resulting return time plots are shown in Figs. 6c and 6d. When moving to more extreme events, characterized by longer return times, the uncertainty in the estimated probabilities increases, although the median of the individual model simulations (not shown) is found to be generally consistent with the observed estimates for extremes with return times of up to 10–20 years, similar to the thresholds used in the attribution analysis. The observations are generally within the modeled range, with the exception of wet extremes with observed return times greater than 20 years, which appear to be rarer in the HadGEM3-A simulations. Such events, however, are not considered in this study. We finally examine the U.K. winter temperature and rainfall dependence on the QBO, the atmospheric circulation pattern of 2015/16, and the ENSO phase [a detailed assessment of the representation of ENSO by

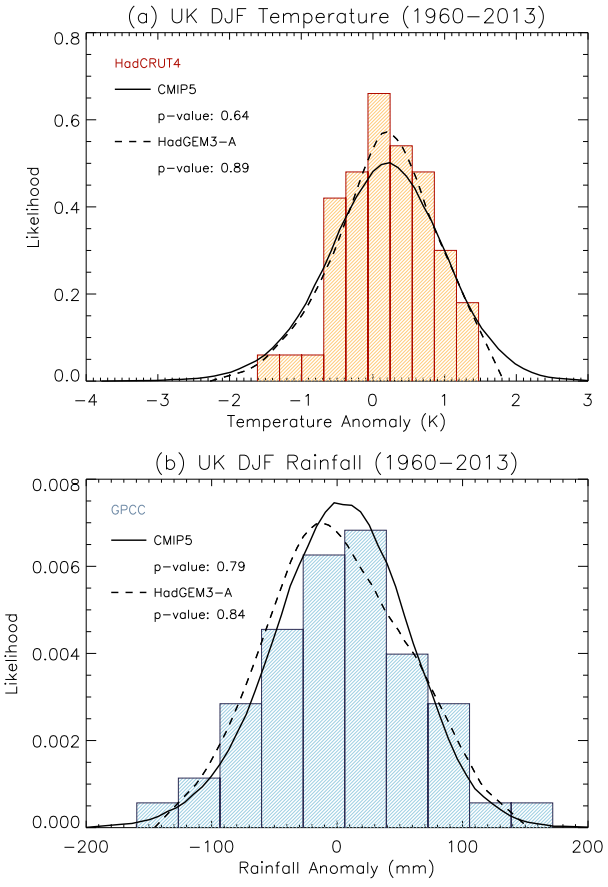

FIG. 5. Normalized distributions of the winter mean (a) temperature and (b) rainfall anomaly in the United Kingdom over the period 1960–2013 estimated with observational data (colored histograms), an ensemble of CMIP5 models (solid black), and an ensemble of 15 HadGEM3-A simulations (dashed black). All simulations include the effect of both natural and anthropogenic forcings. KS tests indicate no significant difference between the modeled PDFs and those from observational data (p values marked on the panels). Anomalies are relative to 1961–90.

CMIP5 models can be found in Bellenger et al. (2014)]. Scatterplots of the observed temperature and rainfall anomalies in recent decades plotted against the corresponding QBO index, the correlation coefficient with the 2015/16 circulation pattern (black box of Fig. 4a), and the ONI are shown in Fig. 7, together with a simple linear fit. Linear fits produced with data from all the model simulations combined (ALL experiment) are also plotted in green. The QBO and circulation dependence are investigated with HadGEM3-A and the ENSO dependence with CMIP5 models as in the subsequent attribution analyses. It is evident that QBO and ENSO have little influence on temperature and rainfall, but the presence of westerly winter flow clearly increases the chances of warm and wet winters in the United Kingdom. It needs to be stressed here that the QBO and ENSO may still affect the chances of extremes as components of large-scale teleconnections (Scaife et al. 2017), but their effect does not appear to be prominent when each factor is considered independently. Some weak trends may still be identified; for example, CMIP5 indicates a moderate increase in precipitation under La Niña conditions, but this is not evident in the observations. On the other hand, testing whether the least squares fit has a zero slope indicates statistically significant trends for the circulation effect (Figs. 7b,e). The modeled trends in this case are in good agreement with the ones computed with NCEP–NCAR data. In conclusion, the model evaluation assessments presented here suggest that both the HadGEM3-A and CMIP5 ensembles are sufficiently good at describing extreme events considered in our attribution analysis. Of course the evaluation is limited to the simulations of the historical climate (ALL) but, as in all attribution studies, we assume the model performance is of the same quality in the hypothetical climate without the effect of human influence (NAT).

4. Attribution

We use samples of modeled U.K. temperature and rainfall to create the ALL and NAT distributions representative of the climate in the winter of 2015/16 and obtain estimates of the likelihood of threshold exceedance. PDFs produced with all the CMIP5 data for the general case (i.e., any possible atmospheric and oceanic states) are shown in Fig. 8. For comparison, the PDFs from the 105-member ensembles generated by the atmospheric model for winter 2015/16 are also plotted. The latter are constrained by the observed SST patterns as prescribed via the boundary conditions. Both CMIP5 and HadGEM3-A show a clear shift in the temperature distribution, which means that human influence has increased the chances of a warm winter in 2015/16. There is less consistency in the case of rainfall, with the coupled models suggesting a shift to wetter conditions and the atmospheric model indicating no major change. Indeed, a KS test suggests that the ALL and NAT rainfall distributions from HadGEM3-A are not significantly different. As will be discussed later, this discrepancy may stem from the prescribed SST patterns for 2015/16 and, more specifically, the NAT boundary conditions that may result in wetter winters in the natural world.

Estimates of the return time of warm and wet winters, defined relative to the 1-in-10-year climatological extremes, were derived with CMIP5 models and HadGEM3-A and are illustrated in Figs. 9 and 10 respectively. The 5%–95% uncertainty range from the bootstrapping procedure is wider in the HadGEM3-A

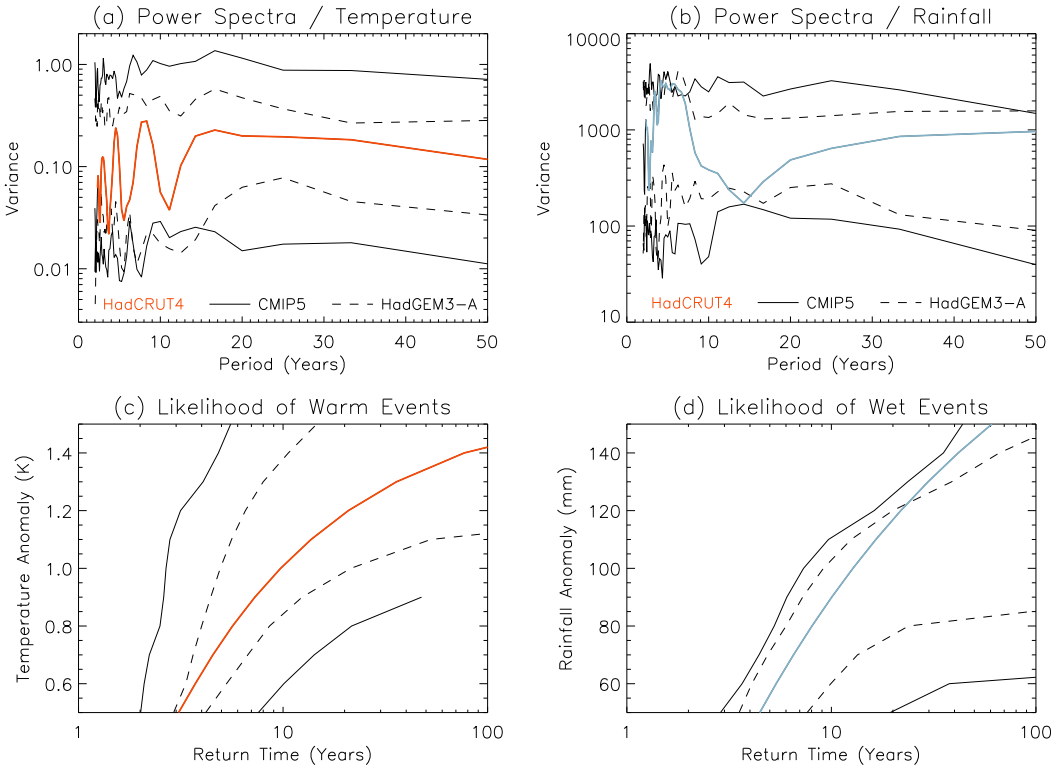

FIG. 6. Power spectra for the winter mean (a) temperature and (b) rainfall in the U.K. over the period 1960–2013 estimated from observations (colored) and plotted together with the range from individual simulations with CMIP5 models (solid black) and HadGEM3-A (dashed black). Similarly, observed estimates of the return time of very (c) warm and (d) wet winters are illustrated together with the range obtained from model simulations. Anomalies are relative to 1961–90.

estimates because of the use of smaller samples, which impacts the precision of extreme probability computations. The leftmost panel sections show return time estimates for the general case from CMIP5 models (Fig. 9) and year 2015/16 from the atmospheric model (Fig. 10). A more than threefold decrease in the return time of warm events is computed with both CMIP5 and the atmospheric model, although HadGEM3-A gives somewhat smaller probabilities (higher return times) for temperature extremes. As also suggested by the distributions in Fig. 8b, while CMIP5 shows a clear decrease in the return time of wet extremes (as winters become wetter), in the HadGEM3-A analysis both the ALL and NAT experiments provide very similar return times (Fig. 10b, leftmost panel section). This difference appears to arise because the NAT return times estimated with HadGEM3-A are smaller than the ones estimated with the CMIP5 models, whereas the ALL return times are in better agreement. It is therefore suggested that the discrepancy may be down to the NAT boundary conditions prescribed in the HadGEM3-A simulations. The NAT SST patterns for winter 2015/16 (Fig. 3b) display a strong gradient in the North Atlantic that may lead to more storms driven over the United Kingdom and hence higher likelihood of rainfall. Interestingly, if the observational delta SST pattern had been employed instead (Fig. 3d), the NAT rainfall probabilities might have looked very different. The reason is that this delta SST pattern shows an area of cooling in central Atlantic (south of Greenland) that, when subtracted from the 2015/16 SSTs, would lead to a much reduced North Atlantic gradient and possibly a reduction in rainfall probability. As in Christidis and Stott (2014) these results suggest that the NAT boundary conditions are the largest uncertainty in attribution studies with atmospheric models that may be critical in regions strongly influenced by the ocean. We also estimated the NAT probability of rainfall extremes with HadGEM3-A data for the last 10 winters (2004–13) of the longer multidecadal simulations, which include a range of different SST patterns, different for every year. Figure 11 shows that when using this wider range of oceanic conditions (rather than the 2015/16 pattern), the estimated return time is consistent with the CMIP5 results. This confirms that the discrepancy between the

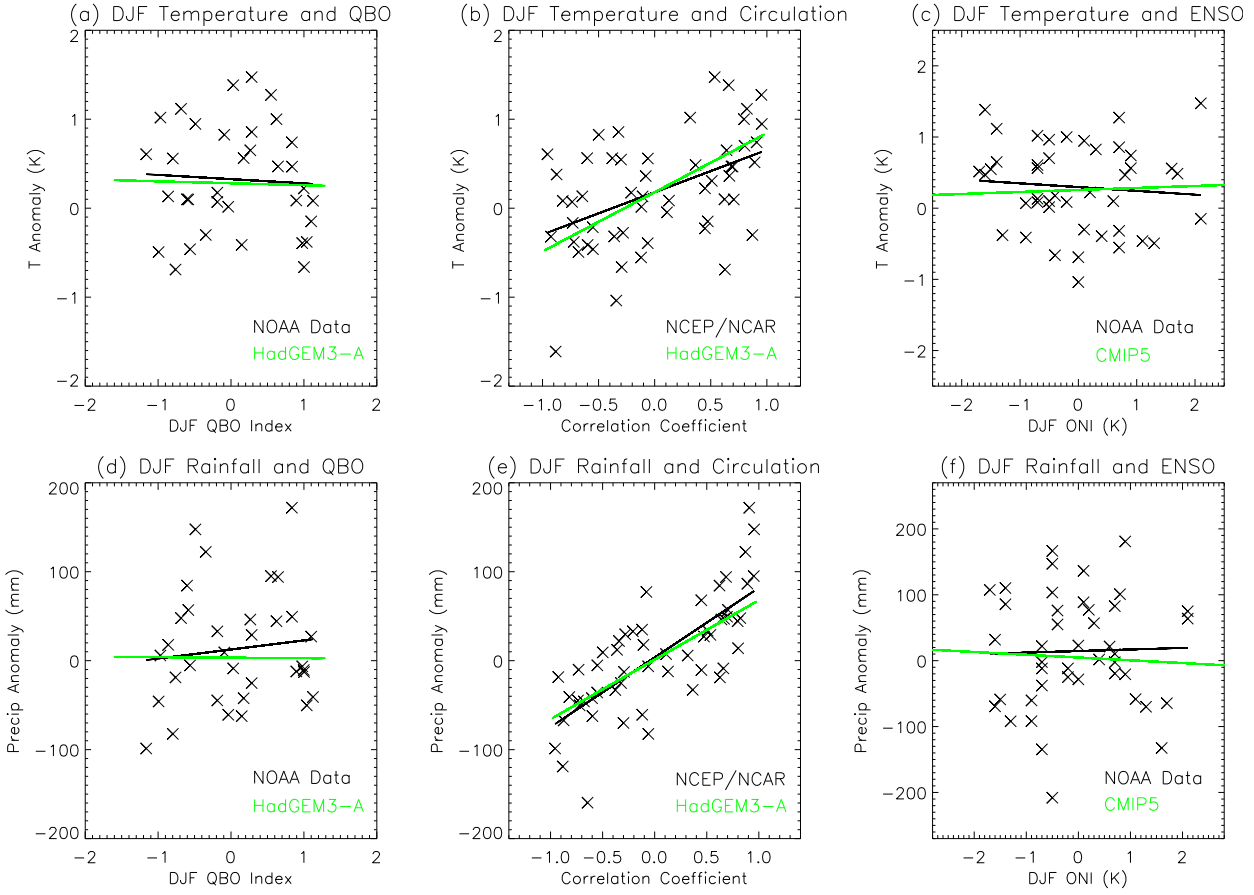

FIG. 7. The relationship between the winter mean temperature in the United Kingdom and (a) the QBO, (b) atmospheric flow similar to 2015/16, and (c) ENSO. (d)–(f) As in (a)–(c), but for rainfall. The crosses correspond to observed temperature and rainfall data and indices from NOAA and NCEP–NCAR datasets. Linear least squares fits are shown in black. Linear fits to data from model simulations are also plotted in green. The period covered is 1979–2012 for QBO and the atmospheric flow and 1971–2013 for ENSO.

CMIP5 and HadGEM3-A probabilities of wet winters is down to the prescribed boundary conditions in the NAT simulations for year 2015/16.

We next use subsamples of model data, as explained in section 2c, to investigate the effect of several possible drivers. First, we partition the CMIP5 data between the ENSO phases to estimate the return times of extremes under El Niño (ONI > 0.5) and La Niña (ONI < -0.5) conditions in the ALL and NAT climate (right panel sections of Fig. 10). ENSO is shown to have hardly any effect on winter U.K. temperature extremes, which have similar return times under both ENSO phases, with or without human influence on the climate. Anthropogenic forcings increase the chances of warm extremes in a similar way under different ENSO phases. The ENSO effect is stronger for winter rainfall and leads to an increase in the chances of wet extremes (smaller return times) during La Niña conditions. Our analysis is based on multimodel ensembles, but we also confirmed this result with individual models and found that for the NAT climate, 60% of the models (20 out of 35) show an increase in wet extremes under La Niña. A similar link between ENSO and European winter precipitation was also found in Pozo-Vázquez et al. (2005). We next look at the effect of the QBO under 2015/16 oceanic conditions by grouping HadGEM3-A simulated winters with strong QBO (index greater than 0.7) and all other winters (index less than 0.7). A comparison with weak QBO conditions (index less than -0.7) was also considered but found not to change the main conclusions while increasing uncertainty due to smaller sample sizes. Estimated return times for different QBO conditions are similar in both the ALL and NAT climate (Fig. 10), although a strong QBO may lead to a small but highly uncertain increase in the chances of warm extremes. The effect of the synoptic pattern in winter 2015/16 (Fig. 4a) is investigated next based on HadGEM3-A simulated winters with high and low pattern correlations. We find that persistent westerly flow strongly influences extreme events (i.e., increases the chances of warm

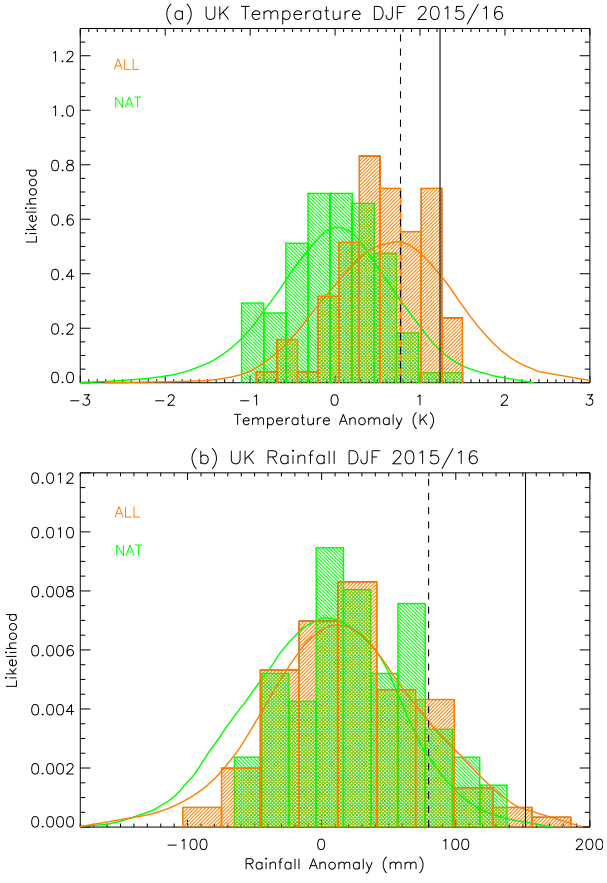

FIG. 8. Normalized distributions of the winter mean (a) temperature and (b) rainfall anomaly representative of winter 2015/16 in the United Kingdom and estimated with (red) and without (green) the effect of human influence using an ensemble of CMIP5 models (solid lines) and an ensemble of 105 HadGEM3-A simulations (histograms). The solid vertical lines mark the observed values in 2015/16 and the dashed vertical lines correspond to 1-in-10-year events in the period 1961–90.

and wet winters) (Fig. 10). This influence is also evident in the NAT climate, although given the synoptic conditions in low correlation winters and the absence of anthropogenic warming, high winter temperatures become so rare that their likelihood cannot be accurately estimated. The plotted return times in Fig. 10 illustrate how both circulation and anthropogenic forcings have a strong impact on the likelihood of extremes. In this case the framing of the attribution question is important, as one may wish to consider human influence in general (irrespective of the circulation effect) or account for the circulation as well. Although both approaches are valid, the latter may provide more useful insights for events like the U.K. winter storms of 2013/14, which also developed under similar large-scale conditions (Christidis and Stott 2015). Finally, we also assessed the effect of initialization by comparing HadGEM3-A-derived return times of extreme events in the actual climate (ALL) with those from GloSea5 initialized forecast simulations. Both ensembles provide very similar estimates for warm and wet events, which suggests that initialization is not vital in attribution studies of these event classes.

Event attribution studies commonly report relative changes in the likelihood of extremes, using metrics like the fraction of attributable risk (Allen 2003) or the risk ratio. Table 2 provides risk ratio estimates that measure the anthropogenic effect on warm and wet U.K. winters, but for different ways of framing the attribution question, namely different classes of events. We present the best estimate (50th percentile) together with the 5%–95% uncertainty range, but mainly focus on the 5th percentile in the discussion below, as the most conservative measure of the effect of human influence. The likelihood of warm events is found to increase by at least a factor of 3–4 for all cases examined here, apart from analyses conditioned on circulation patterns different from 2015/16 or a strong QBO. However, the risk ratio estimates in these two cases are highly uncertain, either because the NAT probabilities are near zero (circulation) or because the samples are too small to yield reliable probability estimates for extremes (QBO). We conclude that even though the prescribed SSTs and prevalent circulation flow may influence the probability of warm winters in the actual and natural climatic regimes, they do not appear to have a strong effect on the relative change in the probability. A three- or fourfold increase in the chances of warm winters is our most conservative estimate for the general case, but also for events conditioned on the 2015/16 oceanic state and synoptic situation. In contrast, there is a marked difference between the risk ratios for wet winters from CMIP5 models and HadGEM3-A. The coupled models indicate an increase in the likelihood of such events due to anthropogenic influence by at least a factor of 1.5–2, independent of the ENSO phase. On the other hand, the 5%–95% uncertainty range of the HadGEM3-A risk ratios encompasses both decreases (ratio estimates less than unity) and increases (ratio estimates greater than unity) in the likelihood of wet events conditioned on prescribed SST patterns and additional possible drivers. While the ALL probabilities in these cases are consistent with those obtained from coupled models, the NAT probabilities, as already discussed, are greater than the CMIP5 estimates and so lead to smaller risk ratios. We therefore conclude that the robustness of the HadGEM3-A findings very much depends on the quality of the boundary conditions employed in the NAT experiment. Using HadGEM3-A to estimate probabilities of wet events for the general case (by concatenating recent years with different oceanic

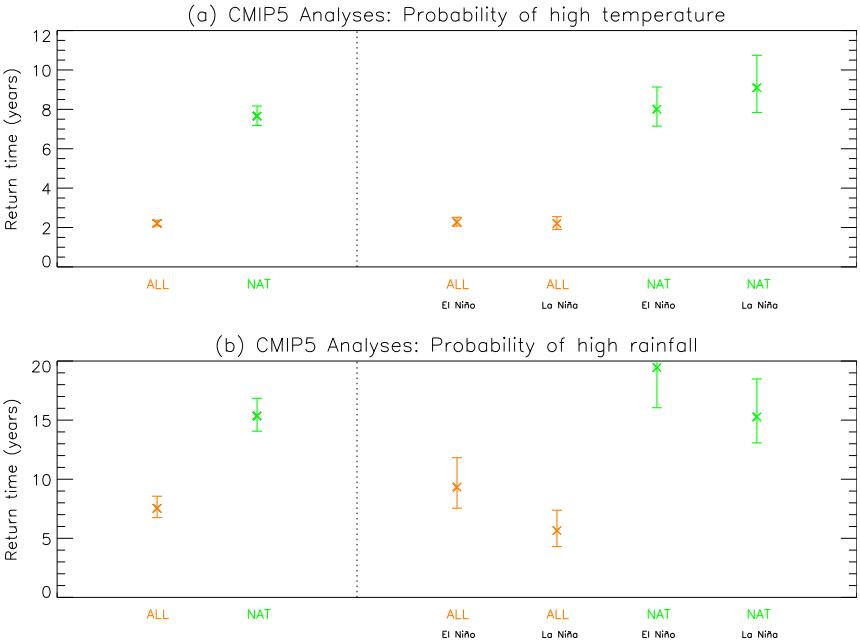

FIG. 9. CMIP5 model estimates of the return time of extremely (a) warm and (b) wet winters in the United Kingdom with (red) and without (green) the effect of anthropogenic forcings. The left section of the panels illustrates the general case (i.e., events occurring under any conditions), while the right section shows results conditioned on the phase of ENSO. Crosses correspond to the best estimate (50th percentile) and whiskers mark the 5%–95% uncertainty range.

conditions), we obtained results consistent with CMIP5 (Fig. 11), which implies that while the model itself is no worse for attribution than the coupled models, analyses conditioned on specific SST patterns will be as good as the boundary conditions they employ. Results for warm events seem to be less sensitive to the boundary conditions. HadGEM3-A probabilities of warm winters are a bit lower than those derived with CMIP5. This, however, is the case not only in the NAT but also in the ALL experiment, which could indicate that the state of the ocean in 2015/16 may somewhat alter the return times relative to the general case, although not the risk ratio. It is possible, for example, that the presence of cold SST anomalies in central Atlantic during DJF 2015/16 (Fig. 3a) in conjunction with a westerly flow may have reduced the likelihood of warm events that year. Therefore, analyses conditioned on the state of the ocean can still convey useful information, but the sensitivity of the results to the NAT boundary conditions needs to be carefully considered.

5. Discussion

Our attribution assessment of winter of 2015/16 in the United Kingdom contributes to the strong evidence that human influence has increased the likelihood of warm extremes and adds to the increasing number of studies indicating changes in the likelihood of wet extremes too (Herring et al. 2016b). It is also consistent with a climatic shift toward warmer and wetter winters in the region indicated by model projections (Murphy et al. 2009; van Oldenborgh et al. 2013, annex I). Anthropogenic forcings are found to increase the chance of exceeding warm winter temperatures that occurred on average once a decade in a recent climatological period (1961–90), by at least a factor of 3–4. The presence of a predominately westerly circulation further increases the likelihood of warm extremes. A more modest increase in the likelihood of 1-in-10-year heavy rainfall climatological extremes of at least a factor of 1.5–2 is also reported, though the precise increase in years when other possible drivers come into play is more difficult to be estimated. While our attribution results are undoubtedly of great interest, this study is not primarily focused on the reference event, but instead uses it to examine the sensitivity of attribution results to different framing choices.

A number of possible drivers of extreme U.K. winters (other than anthropogenic climate change) are considered in this study. Although some of them are known to play a key role in some parts of the world, they are found to have little, if any, impact on the attribution of U.K.

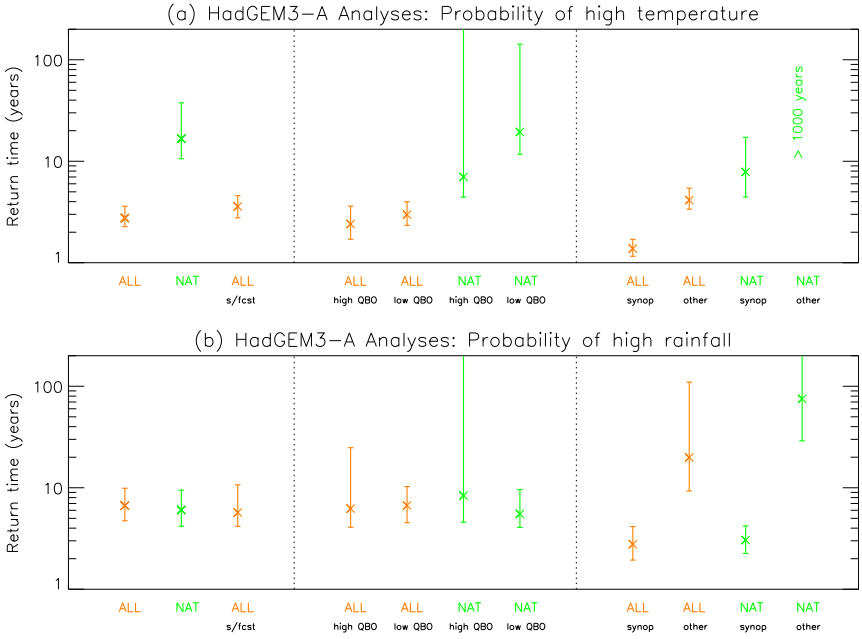

FIG. 10. HadGEM3-A estimates of the return time of extremely (a) warm and (b) wet winters in the United Kingdom with (red) and without (green) the effect of anthropogenic forcings. The left section of the panels illustrates estimates obtained using all available model data for winter 2015/16, which are conditioned on observed SST anomalies. For comparison estimates with GloSea5 initialized simulations (labeled ALL s/fcst) are also shown. The middle section of the panels shows results conditioned on the phase of the QBO. The right section shows results for winters with similar (ALL synop) and dissimilar (ALL other) atmospheric flow to DJF 2015/16. Crosses correspond to the best estimate (50th percentile) and whiskers mark the 5%–95% uncertainty range.

winters. For example, the presence of strong El Niño conditions during the warm winter of 2015/16 was found to have no effect on the likelihood of warm extremes. Of course, it has long been established that the occurrence of extremes in regions worldwide may be favored by a certain phase of ENSO, but this link appears to be more tenuous in the U.K. winter temperatures. Nevertheless, a stronger ENSO influence is suggested on wet events, with their likelihood increasing under La Niña conditions, although such a change is not yet evident in the observations. If this is indeed the case, then El Niño conditions in 2015/16 were not conducive to the observed high rainfall, which, however could have been favored by other drivers such as the synoptic conditions. In terms of framing attribution questions, we find that ENSO did not affect the change in the risk of the reference warm and wet winter due to human influence, despite the fact that it may exert some influence on the likelihood of wet events. The strong westerly phase of the QBO is found to be unlikely to affect the likelihood of warm and wet events. The QBO, however, may still play an important role as part of large-scale dynamical interactions. For example, a known teleconnection between the North Atlantic circulation to the positive phase of El Niño, the westerly phase of the QBO, and a strong stratospheric polar jet enabled a successful forecast of the extreme winter of 2015/16 (Scaife et al. 2017). On the other hand, many attribution studies are mainly

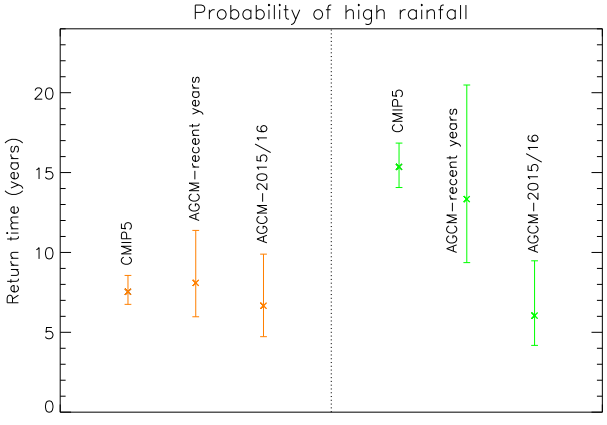

FIG. 11. Estimates of the return time of extremely wet winters in the United Kingdom with (red) and without (green) the effect of anthropogenic forcings computed with CMIP5 models and an AGCM (HadGEM3-A). AGCM estimates are shown for two sets of boundary conditions: one for the range of SSTs in recent years (2004–13) and for the 2015/16 SST pattern. Crosses correspond to the best estimate (50th percentile) and whiskers mark the 5%–95% uncertainty range.

TABLE 2. Anthropogenic effect on the likelihood of warm and wet winters in the United Kingdom.

	Attribution question	Temperature	Rainfall
	What is the change in the likelihood of a warm/wet winter...	Prob(ALL)/Prob (NAT) Best estimate (5%–95% range)	Prob(ALL)/Prob (NAT) Best estimate (5%–95% range)
Coupled models (CMIP5)	in the general case?	3.46 (3.17 to 3.78)	2.02 (1.76 to 2.36)
	in El Niño years?	3.51 (3.00 to 4.14)	2.10 (1.52 to 2.83)
	in El Niña years?	4.14 (3.33 to 5.14)	2.71 (1.97 to 3.77)
AGCM (HadGEM3-A)	for SST anomalies similar to 2015/16?	6.04 (3.60 to 13.71)	0.89 (0.53 to 1.56)
	for winter circulation (and SST anomalies) similar to 2015/16?	5.66 (3.14 to 12.08)	1.11 (0.65 to 1.79)
	for winter circulation different from (but SST anomalies similar to) 2015/16?	>1000 (695 to >1000)	4.20 (0.49 to >1000)
	for winters with strong QBO (and SST anomalies similar to 2015/16)?	3.04 (1.50 to >1000)	1.35 (0.27 to >1000)
	for winters with weak QBO (and SST anomalies similar to 2015/16)?	6.64 (3.59 to 49.75)	0.84 (0.48 to 1.65)

concerned with broader classes of events, for which the QBO, when considered in isolation, may not be a critical factor. Attribution assessments that account for the synergy between individual factors (in this case the QBO, ENSO, and the polar vortex) would require a more stringent class of events to be defined, whereby each factor corresponds to the observed conditions at the time of the event. However, creating a sample of events for such a class by subselecting simulated winters that meet all the necessary criteria would require considerably larger ensembles. In contrast to ENSO and the QBO (examined separately), the dominant winter circulation pattern is found to have a strong influence on the type of extremes considered here.

Persistent warm and humid westerly and southwesterly winds over the United Kingdom are expected to increase the chances of high winter temperature and rainfall in the United Kingdom as demonstrated in this study. Alternative methodologies based on circulation analogs have also been developed to examine the effect of circulation in attribution studies of extreme events (Cattiaux and Yiou 2012; Yiou and Cattiaux 2014). Although circulation is clearly shown to affect the return time of extremes, we again find no strong effect on the relative change (i.e., the changing risk of extremes due to anthropogenic forcings). An important aspect that has not been investigated here is the possibility of dynamical changes under climate change that may make certain atmospheric flows more or less frequent. Vautard et al. (2016) introduced a novel way of separating the thermodynamical and dynamical contributions to the changing odds of extremes and claimed that a third of the increase on the likelihood of the U.K. winter storms of 2013/14 were attributable to dynamical changes. Here we make no attempt to account for any dynamical effect, but consider the same flow pattern in both the ALL and NAT climate assuming no significant change in its frequency in these two types of climate. We suggest that this is a reasonable assumption, based on the work of Christidis and Stott (2015), who identified only a small and not yet robustly established trend in the frequency of a westerly flow pattern similar to the one considered here. The authors of that study examined the modeled frequency of a winter circulation pattern over the United Kingdom similar to the one we consider here and identified a positive and significant trend since 1900, which, however, appears small in the context of internal variability [more discussion and an illustration of results are available in the supplemental material of Christidis and Stott (2015)]. Hence, we consider the thermodynamic response of the climate to external forcings to be essential in event attribution, although consideration of the dynamical response in attribution studies would certainly be an advantage.

Studies with atmospheric models conditioning their attribution assessments on the state of the ocean are inevitably affected by uncertainty in the representation on the ocean temperature in the counterfactual climate without human influence. While the main features of the observed SSTs, such as ENSO-related anomalies, are preserved in the NAT boundary conditions, their magnitude and other general pattern characteristics may vary depending on the delta SST estimate used in the analysis. Here we found that conditioning on the SSTs has little influence on the likelihood of wet events in the ALL experiment, but increases it in the NAT climate. Such an increase is not evident when a range of oceanic states is employed in the NAT experiment, suggesting that the reliability of the result depends on how realistic the underlying delta SST estimate is. The sensitivity to

delta SST has been highlighted as the largest uncertainty in studies with atmospheric models and generally two main approaches have been employed to account for it. The first involves generating multiple NAT ensembles with different possible delta SSTs from individual models. While this would in effect span much of the uncertainty range, it does not help reduce it, if unreliable patterns of the SST change are also utilized. The second approach attempts to improve the representation of the delta SST instead. Better patterns may be obtained by multimodel ensembles that could in principle reduce the effect of errors in single-model estimates, or by making use of observed SST trends. Although we have not used an observational delta SST estimate in our model runs, we find that it indicates some differences from the multimodel pattern and thus conclude that more work is necessary to better account for the uncertainty in the NAT boundary conditions.

Finally, in this paper we only considered methodologies within the popular risk-based framework for event attribution that provides probabilistic assessments for classes of events which share some important characteristics with the event under consideration. A different thread of work has also been proposed that considers the actual event in a deterministic way (Shepherd 2016). This ''storyline'' approach builds up a case for the particular event by estimating the contributions of individual drivers. Both approaches provide useful insights to decision makers. If a specific extreme event becomes a benchmark for resilience, a storyline analysis can be preferable. If, on the other hand, the interest is in protecting against the future occurrence of similar types of events, a risk-based approach may be more useful. Attribution systems built on such risk-based approaches have taken center stage in the development of event attribution science and, moving forward, ongoing research is bringing them closer to operationalization and integration into future climate services.

Acknowledgments. This work was supported by the joint BEIS/Defra Met Office Hadley Centre Climate Programme (GA01101).

REFERENCES

Allen, M., 2003: Liability for climate change. *Nature*, **421**, 891–892, https://doi.org/10.1038/421891a.

Angélil, O., and Coauthors, 2018: On the nonlinearity of spatial scales in extreme weather attribution statements. *Climate Dyn.*, **50**, 2739–2752, https://doi.org/10.1007/s00382-017-3768-9.

Baldwin, M. P., and Coauthors, 2001: The quasi-biennial oscillation. *Rev. Geophys.*, **39**, 179–229, https://doi.org/10.1029/1999RG000073.

Bellenger, H., E. Guilyardi, J. Leloup, M. Lengaigne, and J. Vialard, 2014: ENSO representation in climate models: From CMIP3 to CMIP5. *Climate Dyn.*, **42**, 1999–2018, https://doi.org/10.1007/s00382-013-1783-z.

Black, M. T., and Coauthors, 2016: The weather@home regional climate modelling project for Australia and New Zealand. *Geosci. Model Dev.*, **9**, 3161–3176, https://doi.org/10.5194/gmd-9-3161-2016.

Cattiaux, J., and P. Yiou, 2012: Contribution of atmospheric circulation to remarkable European temperatures of 2011 [in ''Explaining Extreme Events of 2011 from a Climate Perspective'']. *Bull. Amer. Meteor. Soc.*, **93** (7), 1054–1057, https://doi.org/10.1175/BAMS-D-12-00021.1.

Christidis, N., and P. A. Stott, 2014: Change in the odds of warm years and seasons due to anthropogenic influence on the climate. *J. Climate*, **27**, 2607–2621, https://doi.org/10.1175/JCLI-D-13-00563.1.

——, and ——, 2015: Extreme rainfall in the United Kingdom during winter 2013/14: The role of atmospheric circulation and climate change [in ''Explaining Extreme Events of 2014 from a Climate Perspective'']. *Bull. Amer. Meteor. Soc.*, **96** (12), S46–S50, https://doi.org/10.1175/BAMS-ExplainingExtremeEvents2014.1.

——, and ——, 2016: Attribution analyses of temperature extremes using a set of 16 indices. *Wea. Climate Extremes*, **14**, 24–35, https://doi.org/10.1016/j.wace.2016.10.003.

——, ——, A. A. Scaife, A. Arribas, G. S. Jones, D. Copsey, J. R. Knight, and W. J. Tennant, 2013: A new HadGEM3-A based system for attribution of weather- and climate-related extreme events. *J. Climate*, **26**, 2756–2783, https://doi.org/10.1175/JCLI-D-12-00169.1.

——, ——, and F. W. Zwiers, 2015: Fast-track attribution assessments based on pre-computed estimates of changes in the odds of warm extremes. *Climate Dyn.*, **45**, 1547–1564, https://doi.org/10.1007/s00382-014-2408-x.

Ciavarella, A., and Coauthors, 2018: Upgrade of the HadGEM3-A based attribution system to high resolution and a new validation framework for probabilistic event attribution. *Wea. Climate Extremes*, https://doi.org/10.1016/j.wace.2018.03.003, in press.

Gillett, N. P., M. R. Allen, and S. F. B. Tett, 2000: Modelled and observed variability in atmospheric vertical temperature structure. *Climate Dyn.*, **16**, 49–61, https://doi.org/10.1007/PL00007921.

Hauser, M., and Coauthors, 2017: Methods and model dependency of extreme event attribution: The 2015 European drought. *Earth's Future*, **5**, 1034–1043, https://doi.org/10.1002/2017EF000612.

Herring, S. C., M. P. Hoerling, T. C. Peterson, and P. A. Stott, Eds., 2014: Explaining Extreme Events of 2013 from a Climate Perspective. *Bull. Amer. Meteor. Soc.*, **95** (9), S1–S96, https://doi.org/10.1175/1520-0477-95.9.S1.1.

——, ——, J. P. Kossin, T. C. Peterson, and P. A. Stott, Eds., 2015: Explaining Extreme Events of 2014 from a Climate Perspective. *Bull. Amer. Meteor. Soc.*, **96** (12), S1–S172, https://doi.org/10.1175/BAMS-ExplainingExtremeEvents2014.1.

——, A. Hoell, M. P. Hoerling, J. P. Kossin, C. J. Schreck III, and P. A. Stott, Eds., 2016a: Explaining Extreme Events of 2015 from a Climate Perspective. *Bull. Amer. Meteor. Soc.*, **97** (12), S1–S145, https://doi.org/10.1175/BAMS-ExplainingExtremeEvents2015.1.

——, ——, ——, ——, C. J. Schreck III, and P. A. Stott, 2016b: Summary and broader context [in ''Explaining Extreme Events of 2015 from a Climate Perspective'']. *Bull. Amer. Meteor. Soc.*, **97** (12), S141–S145, https://doi.org/10.1175/BAMS-ExplainingExtremeEvents2015.1.

Hewitt, H. T., D. Copsey, I. D. Culverwell, C. M. Harris, R. S. R. Hill, A. B. Keen, A. J. McLaren, and E. C. Hunke, 2011: Design and implementation of the infrastructure of HadGEM3: The next-generation Met Office climate modelling system. *Geosci. Model Dev.*, **4**, 223–253, https://doi.org/10.5194/gmd-4-223-2011.

Kalnay, E., and Coauthors, 1996: The NCEP/NCAR 40-Year Reanalysis Project. *Bull. Amer. Meteor. Soc.*, **77**, 437–471, https://doi.org/10.1175/1520-0477(1996)077<0437:TNYRP>2.0.CO;2.

Karoly, D. J., M. T. Black, A. D. King, and M. R. Grose, 2016: The roles of climate change and El Niño in the record low rainfall in October 2015 in Tasmania, Australia [in "Explaining Extreme Events of 2015 from a Climate Perspective"]. *Bull. Amer. Meteor. Soc.*, **97** (12), S127–S130, https://doi.org/10.1175/BAMS-ExplainingExtremeEvents2015.1.

King, A. D., G. J. van Oldenborgh, D. J. Karoly, S. C. Lewis, and H. Cullen, 2015: Attribution of the record high central England temperature of 2014 to anthropogenic influences. *Environ. Res. Lett.*, **10**, 054002, https://doi.org/10.1088/1748-9326/10/5/054002.

——, D. J. Karoly, and G. J. van Oldenborgh, 2016: Climate change and El Niño increase likelihood of Indonesian heat and drought [in "Explaining Extreme Events of 2015 from a Climate Perspective"]. *Bull. Amer. Meteor. Soc.*, **97** (12), S113–S117, https://doi.org/10.1175/BAMS-ExplainingExtremeEvents2015.1.

Lewis, S. C., and D. J. Karoly, 2015: Are estimates of anthropogenic and natural influences on Australia's extreme 2010–2012 rainfall model-dependent? *Climate Dyn.*, **45**, 679–695, https://doi.org/10.1007/s00382-014-2283-5.

——, ——, and M. Yu, 2014: Quantitative estimates of anthropogenic contributions to extreme national and state monthly, seasonal and annual average temperatures for Australia. *Aust. Meteor. Oceanogr. J.*, **64**, 215–230, https://doi.org/10.22499/2.6403.004.

Lott, F. C., N. Christidis, and P. A. Stott, 2013: Can the 2011 East African drought be attributed to human-induced climate change? *Geophys. Res. Lett.*, **40**, 1177–1181, https://doi.org/10.1002/grl.50235.

——, M. Gordon, R. J. Graham, A. A. Scaife, and M. Vellinga, 2014: Reliability of African climate prediction and attribution across timescales. *Environ. Res. Lett.*, **9**, 104017, https://doi.org/10.1088/1748-9326/9/10/104017.

MacLachlan, C., and Coauthors, 2015: Global seasonal forecast system version 5 (GloSea5): A high-resolution seasonal forecast system. *Quart. J. Roy. Meteor. Soc.*, **141**, 1072–1084, https://doi.org/10.1002/qj.2396.

Morice, C. P., J. J. Kennedy, N. A. Rayner, and P. D. Jones, 2012: Quantifying uncertainties in global and regional temperature change using an ensemble of observational estimates: The HadCRUT4 data set. *J. Geophys. Res.*, **117**, D08101, https://doi.org/10.1029/2011JD017187.

Murphy, J. M., and Coauthors, 2009: UK climate projections science report: Climate change projections. Met Office Hadley Centre Rep., 193 pp.

National Academies of Sciences, Engineering, and Medicine, 2016: *Attribution of Extreme Weather Events in the Context of Climate Change*. The National Academies Press, 186 pp., https://doi.org/10.17226/21852.

Newman, P. A., L. Coy, S. Pawson, and L. R. Lait, 2016: The anomalous change in the QBO in 2015–2016. *Geophys. Res. Lett.*, **43**, 8791–8797, https://doi.org/10.1002/2016GL070373.

Otto, F. E. L., 2016: Extreme events: The art of attribution. *Nat. Climate Change*, **6**, 342–343, https://doi.org/10.1038/nclimate2971.

——, and Coauthors, 2015a: Factors other than climate change, main drivers of 2014/15 water shortage in southeast Brazil [in "Explaining Extreme Events of 2014 from a Climate Perspective"]. *Bull. Amer. Meteor. Soc.*, **96** (12), S35–S40, https://doi.org/10.1175/BAMS-ExplainingExtremeEvents2014.1.

——, E. Boyd, R. G. Jones, R. J. Cornforth, R. James, H. R. Parker, and M. R. Allen, 2015b: Attribution of extreme weather events in Africa: A preliminary exploration of the science and policy implications. *Climatic Change*, **132**, 531–543, https://doi.org/10.1007/s10584-015-1432-0.

Pall, P., T. Aina, D. A. Stone, P. A. Stott, T. Nozawa, A. G. J. Hilberts, D. Lohmann, and M. R. Allen, 2011: Anthropogenic greenhouse gas contribution to flood risk in England and Wales in autumn 2000. *Nature*, **470**, 382–385, https://doi.org/10.1038/nature09762.

Peterson, T. C., P. A. Stott, and S. C. Herring, Eds., 2012: Explaining Extreme Events of 2011 from a Climate Perspective. *Bull. Amer. Meteor. Soc.*, **93** (7), 1041–1067, https://doi.org/10.1175/BAMS-D-12-00021.1.

——, M. P. Hoerling, P. A. Stott, and S. C. Herring, Eds., 2013: Explaining Extreme Events of 2012 from a Climate Perspective. *Bull. Amer. Meteor. Soc.*, **94** (9), S1–S74, https://doi.org/10.1175/BAMS-D-13-00085.1.

Pithan, F., and T. Mauritsen, 2014: Arctic amplification by temperature feedbacks in contemporary climate models. *Nat. Geosci.*, **7**, 181–184, https://doi.org/10.1038/ngeo2071.

Pozo-Vázquez, D., S. R. Gámiz-Fortis, J. Tovar-Pescador, M. J. Esteban-Parra, and Y. Castro-Díez, 2005: El Niño–Southern Oscillation events and associated European winter precipitation anomalies. *Int. J. Climatol.*, **25**, 17–31, https://doi.org/10.1002/joc.1097.

Rayner, N. A., D. E. Parker, E. B. Horton, C. K. Folland, L. V. Alexander, D. P. Rowell, E. C. Kent, and A. Kaplan, 2003: Global analyses of sea surface temperature, sea ice, and night marine air temperature since the late nineteenth century. *J. Geophys. Res.*, **108**, 4407, https://doi.org/10.1029/2002JD002670.

Scaife, A., and Coauthors, 2017: Predictability of European winter 2015/16. *Atmos. Sci. Lett.*, **18**, 38–44, https://doi.org/10.1002/asl.721.

Schaller, N., F. E. L. Otto, G. J. van Oldenborgh, N. R. Massey, S. Sparrow, and M. R. Allen, 2014: The heavy precipitation event of May–June 2013 in the upper Danube and Elbe basins [in "Explaining Extreme Events of 2013 from a Climate Perspective"]. *Bull. Amer. Meteor. Soc.*, **95** (9), S69–S72, https://doi.org/10.1175/1520-0477-95.9.S1.1.

——, and Coauthors, 2016: Human influence on climate in the 2014 southern England winter floods and their impacts. *Nat. Climate Change*, **6**, 627–634, https://doi.org/10.1038/nclimate2927.

Schneider, U., A. Becker, P. Finger, A. Meyer-Christoffer, M. Ziese, and B. Rudolf, 2014: GPCC's new land surface precipitation climatology based on quality-controlled in situ data and its role in quantifying the global water cycle. *Theor. Appl. Climatol.*, **115**, 15–40, https://doi.org/10.1007/s00704-013-0860-x.

Seager, R., and M. Hoerling, 2014: Atmosphere and ocean origins of North American droughts. *J. Climate*, **27**, 4581–4606, https://doi.org/10.1175/JCLI-D-13-00329.1.

Serreze, M. C., and R. G. Barry, 2011: Processes and impacts of Arctic amplification: A research synthesis. *Global Planet. Change*, **77**, 85–96, https://doi.org/10.1016/j.gloplacha.2011.03.004.

Shepherd, T. G., 2016: A common framework for approaches to extreme event attribution. *Curr. Climate Change Rep.*, **2**, 28–38, https://doi.org/10.1007/s40641-016-0033-y.

Shiogama, H., M. Watanabe, Y. Imada, M. Mori, Y. Kamae, M. Ishii, and M. Kimoto, 2014: Attribution of the June–July 2013 heat wave in the southwestern United States. *SOLA*, **10**, 122–126, https://doi.org/10.2151/sola.2014-025.

Stott, P. A., D. A. Stone, and M. R. Allen, 2004: Human contribution to the European heatwave of 2003. *Nature*, **432**, 610–613, https://doi.org/10.1038/nature03089.

——, and Coauthors, 2016: Attribution of extreme weather and climate-related events. *Wiley Interdiscip. Rev.: Climate Change*, **7**, 23–41, https://doi.org/10.1002/wcc.380.

Sweet, W., C. Zervas, S. Gill, and J. Park, 2013: Hurricane Sandy inundation probabilities *today and tomorrow* [in ''Explaining Extreme Events of 2012 from a Climate Perspective'']. *Bull. Amer. Meteor. Soc.*, **94** (9), S17–S20, https://doi.org/10.1175/BAMS-D-13-00085.1.

Takayabu, I., K. Hibino, H. Sasaki, H. Shiogama, N. Mori, Y. Shibutani, and T. Takemi, 2015: Climate change effects on the worst-case storm surge: A case study of Typhoon Haiyan. *Environ. Res. Lett.*, **10**, 064011, https://doi.org/10.1088/1748-9326/10/6/064011.

Taylor, K. E., R. J. Stouffer, and G. A. Meehl, 2012: An overview of CMIP5 and the experiment design. *Bull. Amer. Meteor. Soc.*, **93**, 485–498, https://doi.org/10.1175/BAMS-D-11-00094.1.

van der Wiel, K., and Coauthors, 2017: Rapid attribution of the August 2016 flood-inducing extreme precipitation in south Louisiana to climate change. *Hydrol. Earth Syst. Sci.*, **21**, 897–921, https://doi.org/10.5194/hess-21-897-2017.

van Oldenborgh, G. J., M. Collins, J. Arblaster, J. H. Christensen, J. Marotzke, S. B. Power, M. Rummukainen, and T. Zhou, Eds., 2013: Annex I. Atlas of global and regional climate projections. *Climate Change 2013: The Physical Science Basis*, T. F. Stocker et al., Eds., Cambridge University Press, 1313–1939.

——, F. E. L. Otto, K. Haustein, and H. Cullen, 2015: Climate change increases the probability of heavy rains like those of storm Desmond in the UK—An event attribution study in near-real time. *Hydrol. Earth Syst. Sci. Discuss.*, **12**, 13 197–13 216, https://doi.org/10.5194/hessd-12-13197-2015.

Vautard, R., and Coauthors, 2015: Extreme fall 2014 precipitation in the Cévennes Mountains [in ''Explaining Extreme Events of 2014 from a Climate Perspective'']. *Bull. Amer. Meteor. Soc.*, **96** (12), S56–S60, https://doi.org/10.1175/BAMS-ExplainingExtremeEvents2014.1.

——, P. Yiou, F. Otto, P. Stott, N. Christidis, G. J. van Oldenborgh, and N. Schaller, 2016: Attribution of human-induced dynamical and thermodynamical contribution in extreme weather events. *Environ. Res. Lett.*, **11**, 114009, https://doi.org/10.1088/1748-9326/11/11/114009.

——, and Coauthors, 2018: Evaluation of the HadGEM3-A simulations in view of climate and weather event human influence attribution. *Climate Dyn.*, https://doi.org/10.1007/s00382-018-4183-6, in press.

Yiou, P., and J. Cattiaux, 2014: Contribution of atmospheric circulation to wet southern European winter of 2013 [in ''Explaining Extreme Events of 2013 from a Climate Perspective'']. *Bull. Amer. Meteor. Soc.*, **95** (9), S66–S69, https://doi.org/10.1175/1520-0477-95.9.S1.1.

Zhang, W., and Coauthors, 2016: Influences of natural variability and anthropogenic forcing on the extreme 2015 accumulated cyclone energy in the western North Pacific [in ''Explaining Extreme Events of 2015 from a Climate Perspective'']. *Bull. Amer. Meteor. Soc.*, **97** (12), S131–S135, https://doi.org/10.1175/BAMS-ExplainingExtremeEvents2015.1.